Astrocyte-secreted IL-33 mediates homeostatic synaptic plasticity in the adult hippocampus

Ye Wang[a,b,c,d], Wing-Yu Fu[a,b,c,d], Kit Cheung[a,b,c,d], Kwok-Wang Hung[a,b], Congping Chen[c,e,f], Hongyan Geng[g,h], Wing-Ho Yung[g,h], Jianan Y. Qu[c,e,f], Amy K. Y. Fu[a,b,c,d,i], and Nancy Y. Ip[a,b,c,d,i,1]

[a]Division of Life Science, The Hong Kong University of Science and Technology, Clear Water Bay, Hong Kong, China; [b]Molecular Neuroscience Center, The Hong Kong University of Science and Technology, Clear Water Bay, Hong Kong, China; [c]State Key Laboratory of Molecular Neuroscience, The Hong Kong University of Science and Technology, Clear Water Bay, Hong Kong, China; [d]Hong Kong Center for Neurodegenerative Diseases, Hong Kong, China; [e]Department of Electronic and Computer Engineering, The Hong Kong University of Science and Technology, Clear Water Bay, Hong Kong, China; [f]Center of Systems Biology and Human Health, The Hong Kong University of Science and Technology, Clear Water Bay, Hong Kong, China; [g]School of Biomedical Sciences, Faculty of Medicine, The Chinese University of Hong Kong, Shatin, Hong Kong, China; [h]Gerald Choa Neuroscience Centre, The Chinese University of Hong Kong, Shatin, Hong Kong, China; and [i]Guangdong Provincial Key Laboratory of Brain Science, Disease and Drug Development, HKUST Shenzhen Research Institute, Shenzhen–Hong Kong Institute of Brain Science, 518057, Shenzhen, Guangdong, China

Contributed by Nancy Y. Ip, November 16, 2020 (sent for review October 5, 2020; reviewed by James Bibb and Lin Mei)

Hippocampal synaptic plasticity is important for learning and memory formation. Homeostatic synaptic plasticity is a specific form of synaptic plasticity that is induced upon prolonged changes in neuronal activity to maintain network homeostasis. While astrocytes are important regulators of synaptic transmission and plasticity, it is largely unclear how they interact with neurons to regulate synaptic plasticity at the circuit level. Here, we show that neuronal activity blockade selectively increases the expression and secretion of IL-33 (interleukin-33) by astrocytes in the hippocampal cornu ammonis 1 (CA1) subregion. This IL-33 stimulates an increase in excitatory synapses and neurotransmission through the activation of neuronal IL-33 receptor complex and synaptic recruitment of the scaffold protein PSD-95. We found that acute administration of tetrodotoxin in hippocampal slices or inhibition of hippocampal CA1 excitatory neurons by optogenetic manipulation increases IL-33 expression in CA1 astrocytes. Furthermore, IL-33 administration in vivo promotes the formation of functional excitatory synapses in hippocampal CA1 neurons, whereas conditional knockout of IL-33 in CA1 astrocytes decreases the number of excitatory synapses therein. Importantly, blockade of IL-33 and its receptor signaling in vivo by intracerebroventricular administration of its decoy receptor inhibits homeostatic synaptic plasticity in CA1 pyramidal neurons and impairs spatial memory formation in mice. These results collectively reveal an important role of astrocytic IL-33 in mediating the negative-feedback signaling mechanism in homeostatic synaptic plasticity, providing insights into how astrocytes maintain hippocampal network homeostasis.

interleukin | hippocampal circuit | homeostasis | learning and memory | PSD-95

Synaptic plasticity, the ability of neurons to alter the structure and strength of synapses, is important for the refinement of neuronal circuits in response to sensory experience during development (1) as well as learning and memory formation in adults (2, 3). To maintain the stability of neuronal network activity, the synaptic strength of neurons is modified through a negative-feedback mechanism termed homeostatic synaptic plasticity (4–6). Specifically, inhibiting neuronal activity in cultured neuronal cells or hippocampal slices by pharmacological administration of the sodium channel blocker tetrodotoxin (TTX) increases the strength of excitatory synapses to rebalance network activity (5–7).

The hippocampus, which comprises the cornu ammonis 1 (CA1), CA2, CA3, and dentate gyrus subregions, is important for memory storage and retrieval. In particular, the CA1 subregion constitutes the primary output of the hippocampus, which is thought to be essential for most hippocampus-dependent memories (8, 9). Moreover, experience-driven synaptic changes in the CA1 microcircuitry impact how information is integrated (10, 11). Accordingly, the induction and expression of synaptic plasticity at hippocampal CA1 excitatory synapses are critically dependent on the structural remodeling and composition of synapses as well as functional modifications of pre- and postsynaptic proteins and neurotransmitter receptors (4–6, 12). As such, structural plasticity is a major regulatory mechanism of homeostatic synaptic plasticity in the hippocampal CA1 region. While most excitatory synapses are located at dendritic spines, morphological changes of dendritic spines likely participate in compensatory adaptations of hippocampal network activity and are therefore involved in learning, memory formation (13), and memory extinction (14).

The efficacy of synaptic transmission and the wiring of neuronal circuitry are regulated not only by bidirectional communication between pre- and postsynaptic neurons, but also through the interactions between neurons and their associated glial cells (15–17). Astrocytes, as the most abundant type of glia in the central nervous system, actively regulate synapse formation, function, and maintenance during development and in the adult brain (18–20). However, the molecular basis of astrocyte–neuron communication

Significance

Synaptic plasticity in the hippocampus is important for learning and memory formation. In particular, homeostatic synaptic plasticity enables neurons to restore their activity levels in response to chronic neuronal activity changes. While astrocytes modulate synaptic functions via the secretion of factors, the underlying molecular mechanisms remain unclear. Here, we show that suppression of hippocampal neuronal activity increases cytokine IL-33 release from astrocytes in the CA1 region. Activation of IL-33 and its neuronal ST2 receptor complex promotes functional excitatory synapse formation. Moreover, IL-33/ST2 signaling is important for the neuronal activity blockade-induced increase of CA1 excitatory synapses in vivo and spatial memory formation. This study suggests that astrocyte-secreted IL-33 acts as a negative feedback control signal to regulate hippocampal homeostatic synaptic plasticity.

Author contributions: Y.W., W.-Y.F., A.K.Y.F., and N.Y.I. designed research; Y.W., K.C., K.-W.H., C.C., and H.G. performed research; A.K.Y.F. and N.Y.I. contributed new reagents/analytic tools; Y.W., W.-Y.F., K.C., K.-W.H., C.C., H.G., W.-H.Y., J.Y.Q., A.K.Y.F., and N.Y.I. analyzed data; and Y.W., W.-Y.F., A.K.Y.F., and N.Y.I. wrote the paper with input from all authors.

Reviewers: J.B., University of Alabama at Birmingham; and L.M., Case Western Reserve University.

The authors declare no competing interest.

[1]To whom correspondence may be addressed. Email: boip@ust.hk.

This article contains supporting information online at https://www.pnas.org/lookup/suppl/doi:10.1073/pnas.2020810118/-/DCSupplemental.

Published December 28, 2020.

in synaptic plasticity is largely unknown. Nevertheless, one of the mechanisms by which astrocytes regulate synapses is by secreting factors (21–25); the most well-characterized one is TNFα. Notably, pharmacologically induced deprivation of neuronal activity increases TNFα release from astrocytes, which modulates homeostatic plasticity in both excitatory and inhibitory neurons through regulation of neuronal glutamate and GABA receptor trafficking (24, 26). Further in vivo studies on germline knockout mice support the roles of astrocyte-secreted TNFα in homeostatic adaptations of cortical circuitry during sensory deprivation (27, 28). Another cytokine interleukin-33 (IL-33) is secreted by astrocytes to regulate synapse development in spinal cord and thalamus (29). Nevertheless, it remains largely unknown how astrocytes respond to changes in neuronal activity to regulate homeostatic synaptic plasticity in the hippocampus as well as learning and memory formation.

In this study, we identified IL-33 as an astrocyte-secreted factor which mediates homeostatic synaptic plasticity in the CA1 subregion of adult hippocampus. Pharmacological blockade of neuronal activity or in vivo optogenetic inhibition of CA1 pyramidal neurons stimulates a local increase in the expression and release of IL-33 from the astrocytes. In turn, this astrocyte-secreted IL-33 and its ST2/IL-1RAcP receptor complex mediate the increase of excitatory synapses and neurotransmission in homeostatic synaptic plasticity. Two-photon imaging of CA1 pyramidal neurons in vivo reveals that IL-33 promotes dendritic spine formation through the synaptic recruitment of postsynaptic scaffolding protein PSD-95. Importantly, conditional knockout of IL-33 in astrocytes decreases excitatory synapses in the CA1 subregion, and inhibition of IL-33/ST2 signaling in adult mice abolishes the homeostatic synaptic plasticity in CA1 pyramidal neurons, resulting in impaired spatial memory formation. Hence, our findings collectively show that astrocyte-secreted IL-33 plays an important role in homeostatic synaptic plasticity in the adult hippocampus and spatial memory formation.

Results

IL-33 Is Secreted by Hippocampal CA1 Astrocytes in Response to Neuronal Activity Blockade. To identify astrocyte-secreted factors that potentially regulate homeostatic synaptic plasticity, we examined the differentially expressed genes in mixed neuron–glia hippocampal cultures ("cultured hippocampal cells" hereafter) following neuronal activity blockade with TTX (1 μM), a sodium channel blocker that inhibits action potentials (30, 31). RNA sequencing (RNA-seq) analysis revealed that compared to the control condition (Con), TTX administration to the cultured hippocampal cells induced the differential expression of 2,524 genes, including 1,031 up-regulated and 1,493 down-regulated genes ($\log_2$ fold change ≥ 0.3 or ≤ -0.3, adjusted $P < 0.05$; Dataset S1). Of note, among the up-regulated genes, 54 encode secreted proteins (32), and 6 of them—*Angptl4*, *A2m*, *Olfml1*, *Il33*, *Smpdl3a*, and *Ptn*—were enriched in astrocytes (*SI Appendix*, Fig. S1 and Dataset S2) (33). Among these candidates, IL-33 is a cytokine that maintains cell homeostasis and regulates innate

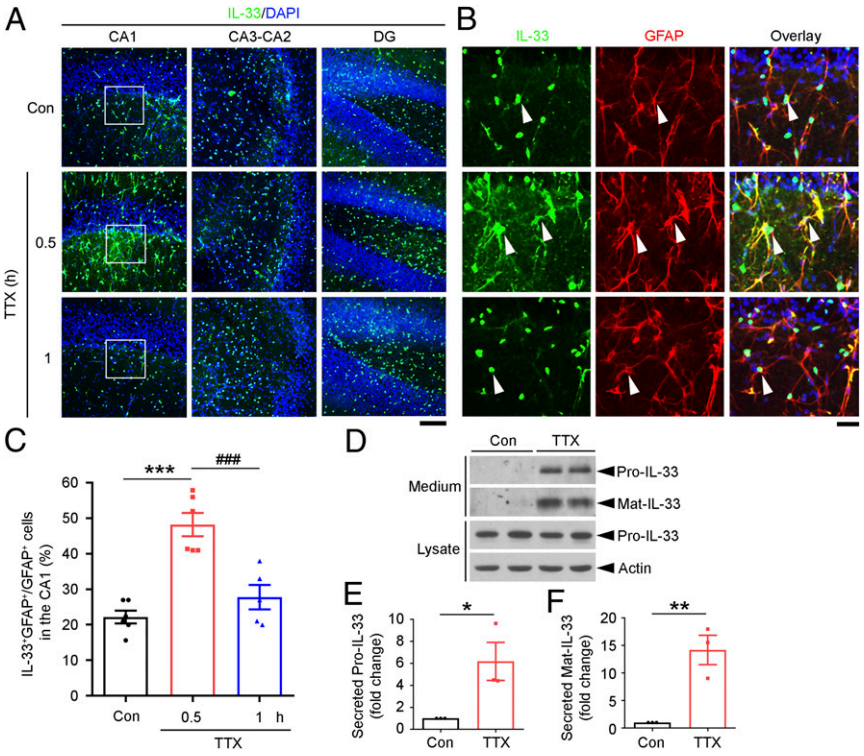

Fig. 1. Neuronal activity blockade by TTX administration induces IL-33 expression and release by astrocytes in the hippocampal cornu ammonis 1 region. (*A–C*) Neuronal activity blockade by TTX induced IL-33 expression in mouse hippocampal astrocytes in a region-specific manner. (*A*) Immunohistochemical analysis of IL-33 expression in hippocampal slices treated with TTX (1 μM) or vehicle (Con). The CA1, CA3–CA2, and dentate gyrus (DG) subregions with DAPI counterstaining are shown. (*B*) Higher-magnification images of the hippocampal CA1 stratum radiatum (white squares in *A*) showing IL-33-expressing astrocytes (labeled with GFAP antibody, white arrowheads) and an overlay including DAPI (blue) counterstaining. (Scale bars, 100 μm in *A* and 25 μm in *B*.) (*C*) Quantification of IL-33-positive astrocytes (IL-33$^+$/GFAP$^+$) (***$P < 0.001$, TTX 0.5 h vs. Con; $^{\#\#\#}P < 0.001$, TTX 1 h vs. 0.5 h; one-way ANOVA; Con: $n = 6$ hippocampal slices; TTX 0.5 h: $n = 6$ hippocampal slices; TTX 1 h: $n = 5$ hippocampal slices; three independent experiments). (*D–F*) Inhibition of neuronal activity by TTX induced IL-33 secretion from mouse hippocampal slices. Acute mouse hippocampal slices were treated with TTX or vehicle (Con) for 1 h. Western blot (*D*) and quantitative analyses of levels of secreted full-length IL-33 (Pro-IL-33) (*E*) and mature IL-33 (Mat-IL-33) (*F*) (Pro-IL-33: *$P < 0.05$; Mat-IL-33: **$P < 0.01$; two-tailed unpaired *t* test; three independent experiments). Values are the mean ± SEM. See also *SI Appendix*, Figs. S1–S3.

immunity (34, 35). Given the expression of IL-33 in brain astrocytes (33, 36) and our previous finding that replenishing IL-33 rescues impaired hippocampal synaptic plasticity in an Alzheimer's disease transgenic mouse model (37), we examined the role of IL-33 in hippocampal synaptic plasticity.

We first investigated whether and which neural cells in the hippocampus responded to neuronal activity blockade in increasing the cellular expression of IL-33. Immunohistochemical analysis was performed following treatment of acute mouse hippocampal slices with TTX at 1 μM for different time periods. We found that TTX administration for 0.5 h significantly increased IL-33 protein expression in the hippocampal CA1 region but not the CA3–CA2 region or dentate gyrus (Fig. 1*A*). In the control condition, IL-33 was expressed in the nuclei of oligodendrocytes and a small portion of astrocytes in the CA1 region (*SI Appendix*, Fig. S2). TTX administration for 0.5 h increased IL-33 protein expression in CA1 astrocytes (i.e., the number of IL-33-expressing astrocytes increased 2.2-fold), whereas the number of IL-33-expressing astrocytes

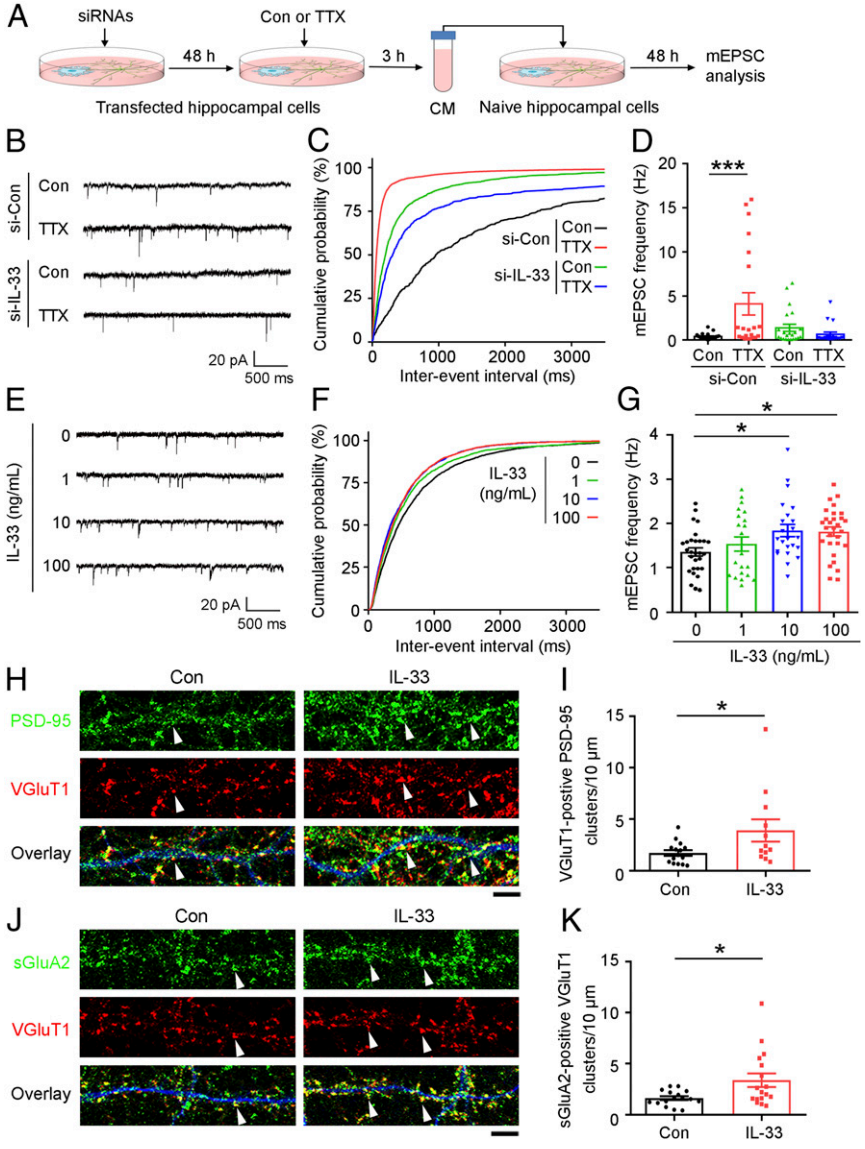

Fig. 2. IL-33 is required for TTX-induced homeostatic synaptic plasticity in cultured rat hippocampal neurons. (*A–D*) IL-33 knockdown abolished the stimulatory effect of TTX to induce homeostatic synaptic plasticity. (*A*) Schematic diagram of the experimental design. Cultured hippocampal cells at 15 to 16 DIV were transfected with IL-33 siRNA (si-IL-33) or control siRNA (Con) for 48 h and treated with TTX or vehicle (Con) for 3 h. The TTX from the conditioned media (CM) was removed by centrifugal filtration (3-kDa cutoff), and the medium was then reconstituted and transferred to naïve cultures of the same growth stage for 48 h before analysis. (*B*) Representative traces of mEPSCs. (*C*) Cumulative probability distributions of mEPSC interevent intervals. (*D*) Quantification of mean mEPSC frequency (***$P < 0.001$, two-way ANOVA; si-Con, Con: $n = 23$ neurons; si-Con, TTX: $n = 21$ neurons; si-IL-33, Con: $n = 22$ neurons; si-IL-33, TTX: $n = 19$ neurons; four independent experiments). (*E–G*) mEPSC analysis of cultured hippocampal cells treated with different doses of IL-33. (*E*) Representative traces of mEPSCs. (*F*) Cumulative probability distributions of mEPSC interevent intervals. (*G*) Quantification of mean mEPSC frequency (*$P < 0.05$, one-way ANOVA; IL-33 at 0, 1, 10, and 100 ng/mL: $n = 29$, 21, 23, and 29 neurons, respectively; three independent experiments). (*H–K*) Immunohistochemical analysis of excitatory synapses in cultured hippocampal neurons after IL-33 administration (100 ng/mL, 24 h). Immunostaining of PSD-95 (*H*) or surface GluA2 (sGluA2) (*J*) and VGluT1 together with MAP2 (blue, to indicate dendritic morphology). (Scale bar, 5 μm.) (*I*) Quantitative analysis of VGluT1-positive PSD-95 clusters (white arrowheads in *H*) (*$P < 0.05$, two-tailed unpaired *t* test; Con: $n = 15$ neurons; IL-33: $n = 12$ neurons; three independent experiments). (*K*) Quantitative analysis of sGluA2-positive VGluT1 clusters (white arrowheads in *J*) (*$P < 0.05$, two-tailed unpaired *t* test; Con: $n = 16$ neurons; IL-33: $n = 17$ neurons; three independent experiments). Values are the mean ± SEM. See also *SI Appendix*, Fig. S4.

returned to the basal level after TTX administration for 1 h (Fig. 1 *B* and *C*). Interestingly, hippocampal slices treated with TTX for 1 h exhibited significantly elevated levels of full-length IL-33 protein (Pro-IL-33) and mature IL-33 protein (Mat-IL-33) in the conditioned media (Fig. 1 *D*–*F*). TTX administration for 3 h also significantly increased IL-33 secretion from cultured hippocampal cells (*SI Appendix*, Fig. S3). These findings suggest that hippocampal neuronal activity blockade induces IL-33 synthesis and stimulates its secretion from hippocampal CA1 astrocytes.

IL-33 Is Necessary and Sufficient for the TTX-Induced Increase of Excitatory Synapses in Homeostatic Synaptic Plasticity. Given that prolonged blockade of neuronal activity increased the expression and secretion of IL-33 protein by CA1 astrocytes, we examined whether IL-33 secreted from these astrocytes is required for homeostatic synaptic plasticity. Accordingly, we transfected cultured hippocampal cells with IL-33-targeting siRNA (si-IL-33) or control siRNA (si-Con). Then, at 17 to 18 days in vitro (DIV) when synaptic connections are developed, we treated the cells with TTX at 1 μM for 3 h. We subsequently collected the conditioned media, removed the TTX by centrifugal filtration, and then transferred the TTX-depleted conditioned media to naïve cultured hippocampal cells derived from the embryos of the same rat and incubated them for 48 h (Fig. 2*A*). Interestingly, the naïve hippocampal cells incubated in this conditioned media collected from cultured si-Con-transfected hippocampal cells exhibited significantly elevated frequency (Fig. 2 *B*–*D*) and amplitude (*SI Appendix*, Fig. S4 *A* and *B*) of miniature excitatory postsynaptic currents (mEPSCs), indicative of the number of excitatory synapses and AMPA receptor abundance at individual synapses, respectively (6, 38). These results suggest that some factor(s) secreted from the TTX-treated hippocampal cell cultures increased excitatory synapse number and synaptic strength. Importantly, the increased mEPSC frequency and amplitude could not be observed if the conditioned media was collected from TTX-treated cultured si-IL-33-transfected hippocampal cells (Fig. 2 *B*–*D* and *SI Appendix*, Fig. S4 *A* and *B*). This indicates that the IL-33 synthesized and secreted by TTX-treated hippocampal cells is necessary for the observed increase in excitatory synaptic transmission in hippocampal neurons, demonstrating that astrocyte-secreted IL-33 plays a role in homeostatic synaptic plasticity.

We subsequently evaluated whether direct IL-33 administration is sufficient to increase excitatory synaptic transmission in hippocampal neurons. While administration of IL-33 at 10 or 100 ng/mL increased mEPSC frequency (Fig. 2 *E*–*G*), it did not significantly alter mEPSC amplitude (*SI Appendix*, Fig. S4 *C* and *D*). These results collectively suggest that IL-33 is both necessary and sufficient to increase the number of excitatory synapses in homeostatic synaptic plasticity.

Next, to investigate the molecular basis of IL-33-stimulated neurotransmission, we treated 19- to 20-DIV cultured hippocampal cells with IL-33 at 100 ng/mL for 24 h. IL-33 administration significantly increased the number of excitatory synapses as indicated by the colabeling of VGluT1 (vesicular glutamate transporter 1, a presynaptic marker) and PSD-95 (postsynaptic density protein 95, a postsynaptic marker) (Fig. 2 *H* and *I*). IL-33 also enhanced the formation of functional AMPA receptors in excitatory synapses as indicated by the increased colocalization of VGluT1 and GluA2 (a subunit of AMPA receptor) (Fig. 2 *J* and *K*). This suggests that the IL-33-stimulated increase in mEPSC frequency is mainly due to an increase in the number of excitatory synapses.

Knockdown of IL-33 Receptor Complex in Neurons Abolishes the IL-33-Stimulated Formation of Excitatory Synapses. The cellular functions of IL-33 are mediated by the activation of its receptor complex, which comprises ST2 and IL-1RAcP (IL-1 receptor accessory protein) (34, 35). Therefore, we examined whether the action of IL-33 in homeostatic synaptic plasticity is mediated by the activation of its cognate receptor complex on hippocampal neurons. Accordingly, we knocked down the IL-33 receptor complex by transfecting shRNA against ST2 (sh-ST2) or IL-1RAcP (sh-IL-1RAcP) in addition to the EGFP construct (to enable the visualization of shRNA-expressing cells for analysis) into 11- to 12-DIV cultured hippocampal cells. At 19 DIV, we treated the cells with IL-33 at 100 ng/mL for 24 h and measured the mEPSCs in the EGFP-expressing neurons. Notably, the shRNA-mediated knockdown of ST2 or IL-1RAcP in hippocampal neurons blocked the IL-33-stimulated increase in mEPSC frequency (Fig. 3 *A*–*C*). Moreover, the shRNA-mediated knockdown of ST2 or IL-1RAcP abolished the IL-33-stimulated increase in the number of excitatory synapses as indicated by the number of endogenous synaptic PSD-95 clusters (labeled with a GFP-tagged PSD-95 intrabody) in the dendritic spine protrusions of tdTomato-labeled shRNA-expressing neurons (Fig. 3 *D* and *E*). These results collectively reveal a role of IL-33 in the induction of functional excitatory synapse formation in hippocampal neurons via the activation of the IL-33 receptor complex. Concordant with the importance of IL-33 and its receptor complex in excitatory synapse formation and neurotransmission, the shRNA-mediated knockdown of ST2 in 20-DIV hippocampal neurons abolished the TTX-stimulated increases in mEPSC frequency and excitatory synaptogenesis (Fig. 3 *F*–*J*). These findings further suggest that IL-33/ST2-dependent signaling is important for homeostatic synaptic plasticity.

IL-33 Enhances Excitatory Synapse Formation by Promoting the Synaptic Recruitment of PSD-95. Given that IL-33 administration increased the number of excitatory synapses, we examined the molecular basis by which IL-33 enhances excitatory synapse formation. As a major scaffold protein at excitatory synapses, PSD-95 is a critical regulator that organizes glutamatergic postsynaptic signaling in excitatory synaptogenesis (39–41). PSD-95 interacts with transmembrane proteins at synapses, including receptors, ion channels, and enzymes, mainly via interactions of its PDZ domains with the C-terminal PDZ-binding motifs of these proteins (39, 42). As IL-1RAcP contains several potential class I PDZ-binding motifs (i.e., X-S/T-X-V/L) (43) at its C terminus, we examined whether IL-1RAcP interacts with PSD-95 by overexpressing ST2, IL-1RAcP, and PSD-95 in HEK293T cells. While we did not detect interactions of these overexpressed proteins at the basal level, administration of IL-33 at 100 ng/mL stimulated the interaction of ST2 with IL-1RAcP to form the heterodimeric receptor complex at 15 min and subsequently induced the binding of PSD-95 to the receptor complex at 1 h (*SI Appendix*, Fig. S5*A*). In cultured rat hippocampal cells, IL-33 administration for 1 h also stimulated the binding of PSD-95 to the IL-33 receptor complex as indicated by an increase (41%) in its interaction with IL-1RAcP (*SI Appendix*, Fig. S5*B*). IL-33 administration also increased the level of PSD-95 in the synaptosomal fractions of cultured hippocampal cells by 76% (Fig. 4*A*). Time-lapse confocal imaging of cultured hippocampal cells expressing PSD-95–GFP revealed that the clustering of PSD-95 in the dendritic spine protrusions labeled with GFP increased significantly by 19% 2 h after administration of IL-33 at 100 ng/mL, indicating that IL-33 enhances the targeting of PSD-95 to dendritic spines (*SI Appendix*, Fig. S6).

The synaptic accumulation of PSD-95 is dependent on its phosphorylation (44–47), especially that at Ser295, which regulates its synaptic abundance and AMPA receptor localization (44). Therefore, we examined the effects of IL-33 on PSD-95 phosphorylation at Ser295. Accordingly, IL-33 administration in cultured hippocampal neural cells increased the phosphorylation of PSD-95 at Ser295 at 1 h, concomitant with the activation of p38 and CaMKII (*SI Appendix*, Fig. S7*A*), which are the downstream kinases of the ST2–IL-1RAcP signaling complex.

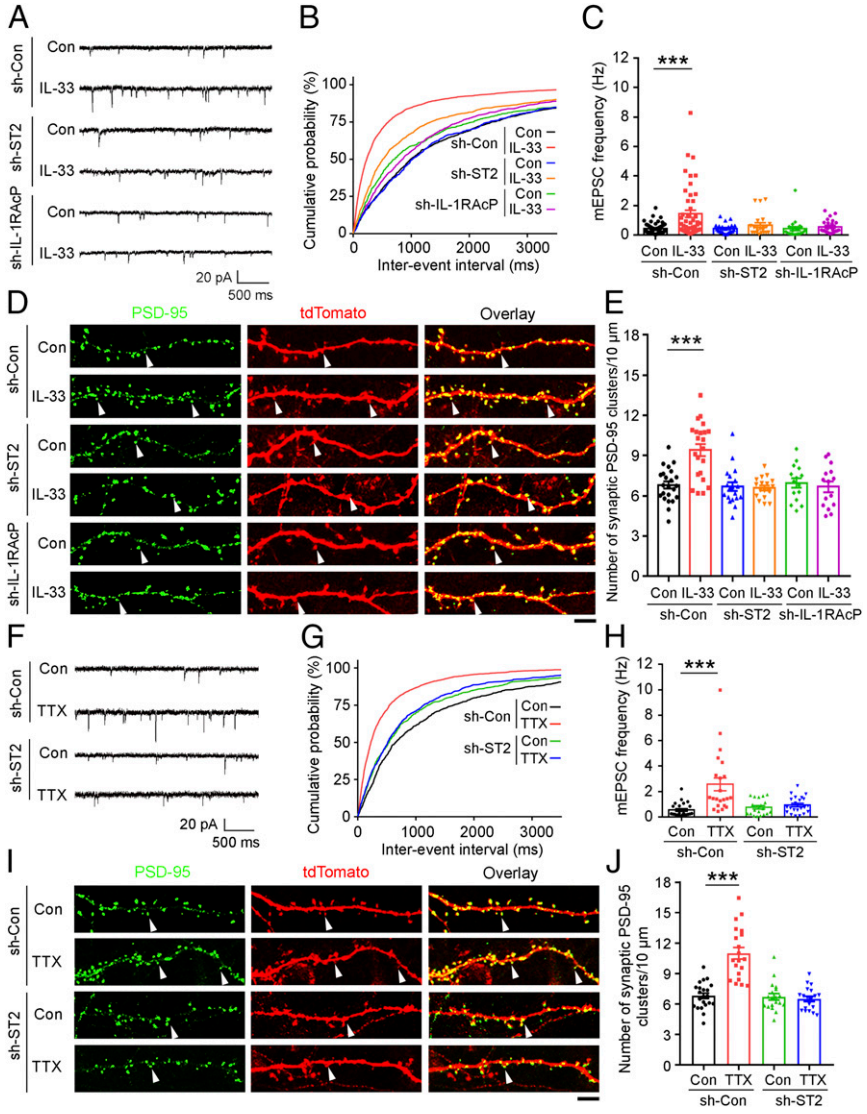

Fig. 3. IL-33 regulates homeostatic plasticity through the activation of its ST2/IL-1RAcP neuronal receptor complex. (*A–E*) Knockdown of ST2 (sh-ST2) or IL-1RAcP (sh-IL-1RAcP) in cultured hippocampal neurons abolished the IL-33-induced increase in excitatory synaptic transmission and the number of synaptic PSD-95 clusters. (*A*) Representative traces of mEPSCs. (*B*) Cumulative probability distributions of mEPSC interevent intervals. (*C*) Quantification of mean mEPSC frequency (***$P < 0.001$, two-way ANOVA; sh-Con, Con: $n = 55$ neurons; sh-Con, IL-33: $n = 49$ neurons; sh-ST2, Con: $n = 23$ neurons; sh-ST2, IL-33: $n = 22$ neurons; sh-IL-1RAcP, Con: $n = 22$ neurons; sh-IL-1RAcP, IL-33: $n = 24$ neurons). (*D*) Representative images of endogenous PSD-95 clusters (labeled with GFP-tagged PSD-95 intrabody) in tdTomato-expressing hippocampal neurons. White arrowheads indicate endogenous PSD-95 clusters in dendritic spine protrusions. (Scale bar, 5 μm.) (*E*) Quantification of synaptic PSD-95 clusters (***$P < 0.001$, two-way ANOVA; sh-Con, Con: $n = 23$ neurons; sh-Con, IL-33: $n = 22$ neurons; sh-ST2, Con: $n = 19$ neurons; sh-ST2, IL-33: $n = 18$ neurons; sh-IL-1RAcP, Con or IL-33: $n = 15$ neurons). (*F–J*) Cultured hippocampal neural cells were transfected with sh-ST2 or sh-Con and treated with TTX for 48 h before mEPSC analysis (*F–H*) or immunocytochemical analysis (*I* and *J*). (*F*) Representative traces of mEPSCs. (*G*) Cumulative probability distributions of mEPSC interevent intervals. (*H*) Quantification of mean mEPSC frequency (***$P < 0.001$, two-way ANOVA; sh-Con, Con: $n = 25$ neurons; sh-Con, TTX: $n = 22$ neurons; sh-ST2, Con: $n = 20$ neurons; sh-ST2, TTX: $n = 22$ neurons). Representative images (*I*) and quantification (*J*) of synaptic PSD-95 clusters (***$P < 0.001$, two-way ANOVA; sh-Con, Con: $n = 23$ neurons; sh-Con, TTX: $n = 20$ neurons; sh-ST2, Con or TTX: $n = 19$ neurons). (Scale bar, 5 μm.) All experiments were performed in triplicates. Values are the mean ± SEM.

Moreover, inhibiting p38 or CaMKII activity abolished the IL-33-stimulated increases in synaptic PSD-95 and excitatory synaptic transmission (*SI Appendix*, Fig. S7 *B–F*). These results collectively suggest that IL-33/ST2/IL-1RAcP signaling enhances excitatory synapse formation via the phosphorylation-dependent synaptic accumulation of PSD-95.

IL-33 Enhances Excitatory Synapse Formation and Synaptic Transmission in the Mouse Hippocampus. Given that IL-33 plays a role in synapse formation and neurotransmission in vitro, we next examined the effects of IL-33 administration on hippocampal excitatory synapses in vivo. In young adult mice (i.e., 3-mo-old C57 mice), administration of IL-33 at 200 ng for 4 h increased the PSD-95 level in the synaptosomal fractions prepared from the hippocampal tissues by 56% (Fig. 4*B*). We subsequently employed a cutting-edge two-photon, adaptive optics microscopy technique (48, 49) to perform in vivo time-lapse imaging of apical dendrites in hippocampal CA1 neurons in the IL-33-treated mice. Labeling with a GFP-tagged PSD-95 intrabody revealed that IL-33 administration stimulated the accumulation of endogenous PSD-95 clusters at dendritic spine protrusions in the CA1 hippocampal neurons (Fig. 4*C*). This indicates that IL-33 administration in vivo stimulates the recruitment of PSD-95 to the postsynaptic structures of CA1 neurons. Concomitant with the enhanced synaptic localization of PSD-95 in

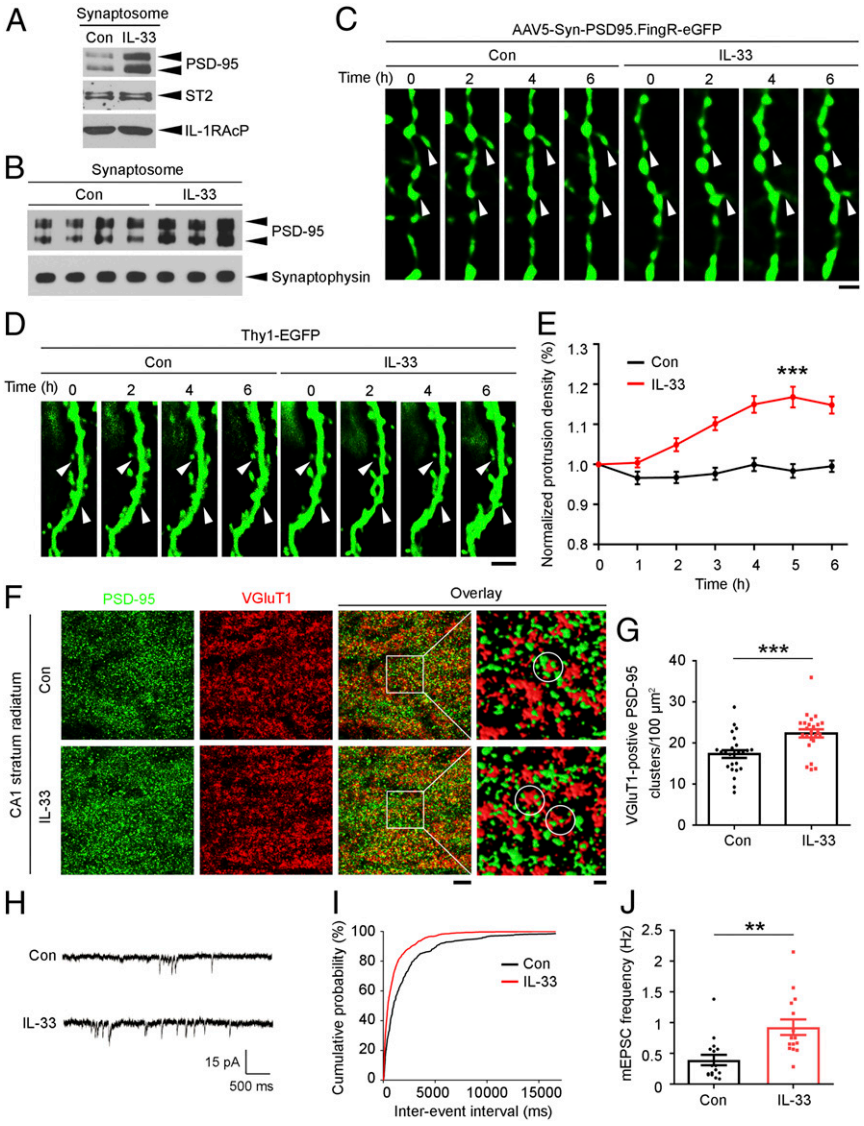

Fig. 4. IL-33 promotes excitatory synaptogenesis by enhancing PSD-95 accumulation at synapses. (*A* and *B*) Western blot analysis of PSD-95 in the synaptosomes of IL-33-treated cultured hippocampal neurons (*A*) and hippocampi from 3-mo-old C57 mice (*B*). (*C*) Time-lapse images showing GFP-labeled PSD-95 clusters on the dendritic spines (white arrowheads) of hippocampal CA1 pyramidal neurons after vehicle (Dulbecco's phosphate-buffered saline [DPBS]; Con) or IL-33 (200 ng) injection. (Scale bar, 2 μm.) (*D* and *E*) IL-33 increased the number of dendritic protrusions in the CA1 pyramidal neurons of 3-mo-old C57 mice. (*D*) Time-lapse images showing morphological changes in the dendritic spines (white arrowheads) of EGFP-expressing dendrites. (Scale bar, 5 μm.) (*E*) Quantification of normalized dendritic protrusion density (***$P < 0.001$, 5 h IL-33 vs. Con; two-tailed unpaired *t* test; Con: $n = 35$ dendrites; IL-33: $n = 42$ dendrites; four mice per group). (*F* and *G*) Immunohistochemical analysis of PSD-95 and VGluT1 in the hippocampal CA1 stratum radiatum subregion after administration of IL-33 (200 ng, 4 h). (*F*) Representative images including overlay images (Scale bar on *Left*, 5 μm.) and higher-magnification segmented images showing PSD-95 and VGluT1 clusters (Scale bar on *Right*, 1 μm.). White circles indicate VGluT1-positive PSD-95 clusters. (*G*) Quantification of VGluT1-positive PSD-95 clusters (***$P < 0.001$, two-tailed unpaired *t* test; Con: $n = 25$ images; IL-33: $n = 24$ images; three mice per group). (*H–J*) Increased excitatory synaptic transmission in hippocampal CA1 pyramidal neurons in 3-mo-old C57 mice treated with IL-33 (200 ng, 4 h). (*H*) Representative traces of mEPSCs recorded in hippocampal slices. (*I*) Cumulative probability distributions of mEPSC interevent intervals. (*J*) Quantification of mean mEPSC frequency (**$P < 0.01$, two-tailed unpaired *t* test; Con: $n = 16$ neurons; IL-33: $n = 15$ neurons; three mice per group). Values are the mean ± SEM. See also *SI Appendix*, Figs. S5–S8.

dendritic spine protrusions, in vivo time-lapse imaging of IL-33-treated Thy1-EGFP mice (a widely used mouse model for two-photon imaging of dendritic spine morphology) (50–52) showed that IL-33 injection for 4 to 6 h significantly increased the dendritic spine protrusion density (Fig. 4 *D* and *E*), suggesting that IL-33 also enhances the formation of dendritic spine protrusions in hippocampal CA1 neurons in vivo. Subsequent immunohistochemical analysis of the brain sections from IL-33-treated mice showed that IL-33 administration significantly increased the number of VGluT1-positive PSD-95 clusters in the hippocampal CA1 stratum radiatum subregion (Fig. 4 *F* and *G*), which contains most CA3–CA1 excitatory synapses. Moreover, IL-33 administration significantly increased mEPSC frequency in CA1 pyramidal neurons from acute hippocampal slices of adult mouse (Fig. 4 *H–J*) without affecting mEPSC amplitude (*SI Appendix*, Fig. S8). Thus, these results indicate that IL-33 enhances the formation of structural and functional excitatory synapses as well as synaptic transmission in CA1 pyramidal neurons in the adult mouse hippocampus in vivo.

In Vivo Inhibition of Hippocampal Neuronal Activity Increases IL-33 Expression in CA1 Astrocytes. To confirm that the level of astrocytic IL-33 is regulated by neuronal activity in the mouse hippocampus

in vivo, we expressed halorhodopsin (NpHR-YFP) under the control of the CaMKIIα promoter in the hippocampal CA1 excitatory pyramidal neurons in adult mice to enable the light-stimulated silencing of action potential firing (53, 54) (Fig. 5*A* and *SI Appendix*, Fig. S9*A*). Consistent with previous findings (55, 56), optogenetic stimulation of NpHR-expressing excitatory neurons in the hippocampal CA1 region silenced their neuronal activity as indicated by the decreased nuclear expression of neuronal activity-regulated c-Fos protein relative to that in unstimulated, NpHR-expressing control neurons (*SI Appendix*, Fig. S9 *B* and *C*). Interestingly, the IL-33 protein level increased in the CA1 astrocytes in the optogenetically stimulated, NpHR-expressing mice, whereas such increase was not observed in the unstimulated, NpHR-expressing or the optogenetically stimulated, GFP-expressing mice (Fig. 5 *B*–*D*). Thus, inhibiting the activity of CA1 hippocampal pyramidal neurons increased IL-33 protein expression in the neighboring astrocytes.

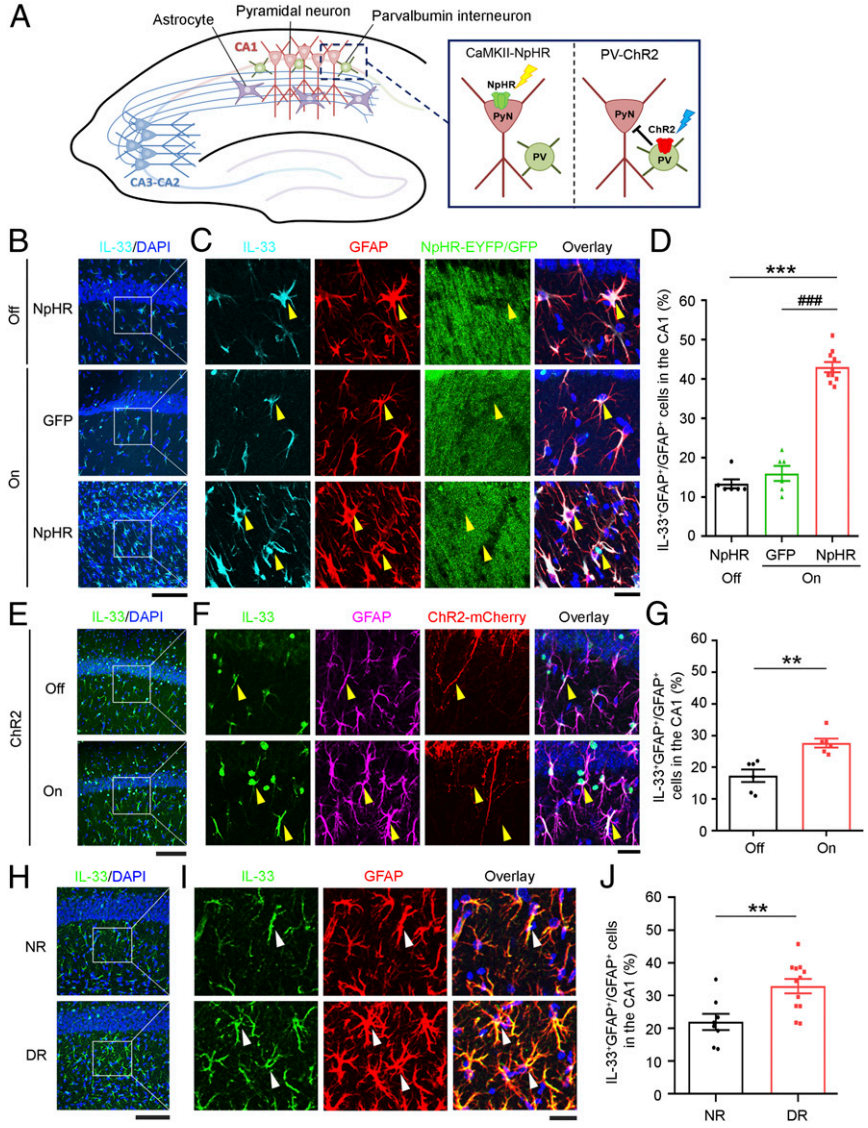

Fig. 5. Inhibition of hippocampal neuronal activity in adult mice increases the IL-33 protein level in CA1 astrocytes. (*A*) Schematic diagram of the experimental design for the optogenetic manipulation of neuronal activity in the hippocampal CA1 microcircuitry. (*B*) Immunohistochemical analysis of IL-33 and DAPI counterstaining in the hippocampal CA1 region in adult mice expressing CamKII-NpHR (halorhodopsin) or GFP without (off) or with (on) 1-h laser stimulation. (*C*) Higher-magnification images showing IL-33-expressing astrocytes (yellow arrowheads) and an overlay with DAPI counterstaining in the CA1 stratum radiatum subregion. (Scale bars, 100 μm in *B* and 25 μm in *C*.) (*D*) Quantification of IL-33-positive astrocytes (***$P < 0.001$, on/NpHR vs. off/NpHR; ###$P < 0.001$, on/NpHR vs. on/GFP; one-way ANOVA; off/NpHR and on/GFP: $n = 6$ brain sections from three mice per group; on/NpHR: $n = 10$ brain sections from five mice). (*E*) Immunohistochemical analysis of IL-33 and DAPI counterstaining in the hippocampal CA1 region in adult mice expressing PV-ChR2 (channelrhodopsin-2) without (off) or with (on) 1-h laser stimulation. (*F*) Higher-magnification images showing IL-33-expressing astrocytes (yellow arrowheads) and an overlay with DAPI counterstaining. (Scale bars, 100 μm in *E* and 25 μm in *F*.) (*G*) Quantification of IL-33-positive astrocytes (**$P < 0.01$, two-tailed unpaired *t* test; $n = 6$ brain sections from three mice per group). (*H*–*J*) Dark rearing increased IL-33 protein levels in astrocytes in the hippocampal CA1 stratum radiatum subregion in mice. Hippocampal samples were collected from normally reared (NR) and dark-reared (DR) mice after the eye-opening period on postnatal day 15. (*H*) Immunohistochemical analysis of IL-33 and DAPI counterstaining in the hippocampal CA1 region. (*I*) Higher-magnification images showing IL-33-expressing astrocytes (white arrowheads) and an overlay with DAPI counterstaining. (Scale bars, 100 μm in *H* and 25 μm in *I*.) (*J*) Quantification of IL-33-positive astrocytes (**$P < 0.01$, two-tailed unpaired *t* test; NR: $n = 8$ brain sections from three mice; DR: $n = 12$ brain sections from four mice). Values are the mean ± SEM. See also *SI Appendix*, Figs. S9–S11.

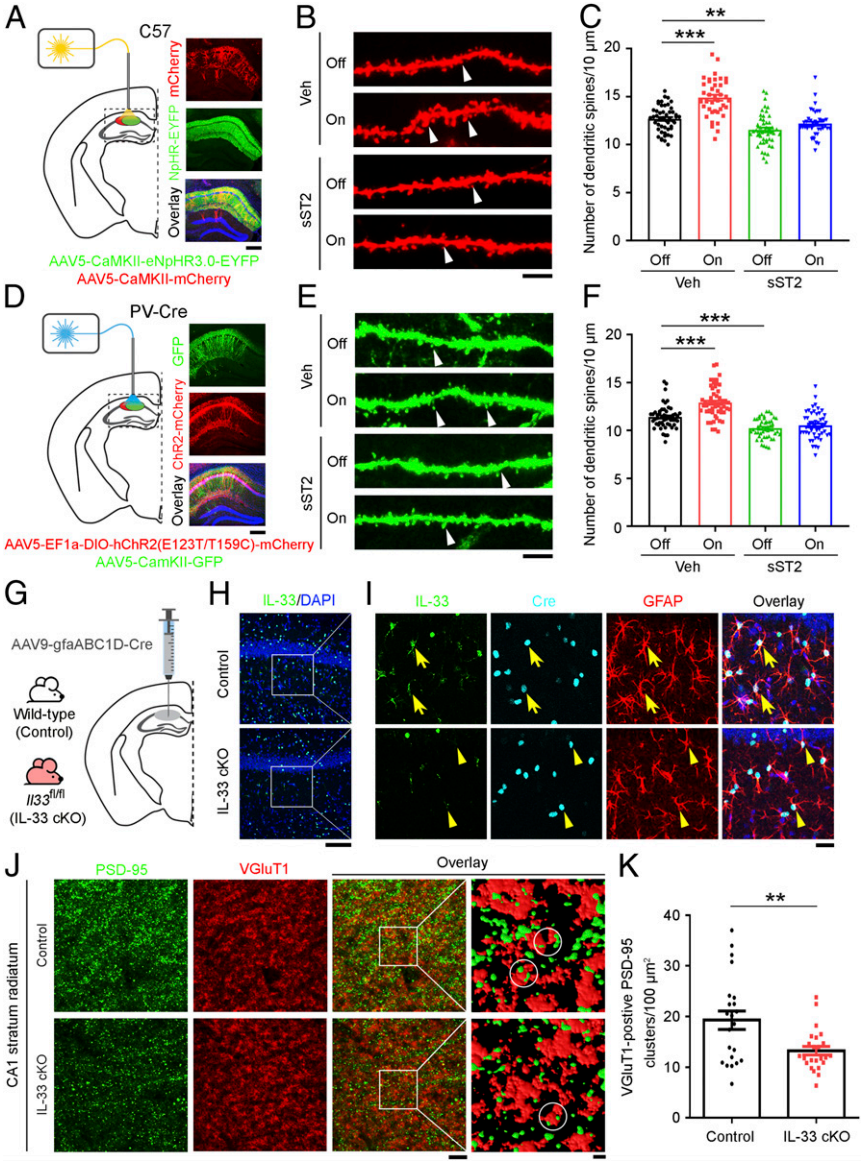

Fig. 6. IL-33/ST2 signaling is required for neuronal activity blockade-induced excitatory synapse formation in the hippocampal CA1 microcircuitry. (*A* and *D*) Generation of (*A*) C57 mice expressing mCherry and NpHR-EYFP viruses in CaMKII-positive pyramidal neurons and (*D*) PV-Cre mice expressing GFP virus in CaMKII-positive pyramidal neurons and ChR2-mCherry virus in parvalbumin (PV)-positive interneurons, respectively, in the hippocampal CA1 region (*Left*). Representative images: mCherry, EYFP, and overlay with DAPI (blue) counterstaining (*Right* in *A*); GFP, mCherry, and overly with DAPI (blue) counterstaining (*Right* in *D*). (Scale bars, 250 μm.) Mice with (*B*) hippocampal CA1 CaMKII-positive pyramidal neurons expressing mCherry/NpHR-EYFP or (*E*) hippocampal CA1 CaMKII-positive pyramidal neurons expressing GFP and PV-positive interneurons expressing ChR2-mCherry viruses, were administered murine recombinant soluble ST2 (sST2) protein (0.13 ng/h) or human IgG Fc fragment (Veh) for 8 d via miniosmotic pumps followed by light stimulation (1 h). Dendritic spine morphology was examined at 8 h later. Off: without light stimulation; on: with light stimulation. Representative images of dendritic spine morphology labeled with mCherry (*B*) and EGFP (*E*). White arrowheads indicate dendritic spines. (Scale bars, 5 μm.) (*C*) Quantification of dendritic spines in mCherry-expressing dendrites in *B* (**$P < 0.01$, ***$P < 0.001$, two-way ANOVA; Veh, off: $n = 49$ dendrites from five mice; Veh, on: $n = 40$ dendrites from five mice; sST2, off: $n = 48$ dendrites from five mice; sST2, on: $n = 41$ dendrites from four mice). (*F*) Quantification of dendritic spines in GFP-expressing dendrites in *E* (***$P <$ 0.001, two-way ANOVA; Veh, off: $n = 53$ dendrites from five mice; Veh, on: $n = 54$ dendrites from six mice; sST2, off: $n = 48$ dendrites from six mice; sST2, on: $n = 51$ dendrites from six mice). (*G–K*) Conditional knockout of IL-33 in hippocampal astrocytes decreased the number of excitatory synapses in CA1 subregion. (*G*) Experimental design. CA1 astrocyte-specific knockout of IL-33 (IL-33 cKO) was achieved by injecting the AAV9-gfaABC1D-Cre virus into the hippocampal CA1 region of the *Il33* floxed ($Il33^{fl/fl}$) mice; the age-matched wild-type mice injected with the virus served as the control. (*H*) Immunohistochemical analysis of IL-33 and DAPI counterstain in the hippocampal CA1 region. (*I*) Higher magnification images showing the IL-33, Cre and GFAP expression, and overlay including DAPI counterstain. Yellow arrows indicate IL-33-positive astrocytes, and yellow arrowheads indicate the absence of IL-33 expression in Cre-expressing astrocytes. (Scale bars, 100 μm in *H* and 25 μm in *I*.) (*J*) Immunohistochemical analysis of PSD-95 and VGluT1 in the hippocampal CA1 stratum radiatum region (Scale bar on *Left*, including an overlay image, 5 μm.) and higher-magnification segmented images showing the PSD-95 and VGluT1 clusters (Scale bar on *Right*, 1 μm.). White circles indicate the VGluT1-positive PSD-95 clusters. (*K*) Quantification of VGluT1-positive PSD-95 clusters (**$P < 0.01$, two-tailed unpaired *t* test; control: $n = 22$ images; IL-33 cKO: $n = 24$ images; four mice per group). Values are the mean ± SEM.

Within the hippocampal CA1 microcircuitry, distinct types of GABAergic interneurons form local connections with pyramidal neurons in a domain-specific manner; the activity of these pyramidal neurons can be suppressed by the activation of their neighboring interneurons (57, 58). Therefore, in addition to directly silencing CA1 excitatory neurons, we suppressed the activity of CA1 excitatory neurons by optogenetically activating parvalbumin (PV) interneurons expressing ChR2 (channelrhodopsin-2) (Fig. 5*A* and *SI Appendix*, Fig. S10*A*) (59). The optogenetically stimulated PV neurons exhibited increased activity as indicated by increased nuclear c-Fos expression, whereas their neighboring excitatory pyramidal neurons exhibited suppressed activity as indicated by a concurrent decrease in nuclear expression of c-Fos (*SI Appendix*, Fig. S10 *B* and *C*). Notably, the suppression of CA1 excitatory neuronal activity using this approach also significantly increased IL-33 protein expression in the surrounding astrocytes (Fig. 5 *E*–*G*). These results collectively suggest that astrocytes in the CA1 stratum radiatum sense the suppression of activity of local excitatory neurons to regulate IL-33 synthesis and secretion.

To determine if astrocytic expression of IL-33 is regulated by neuronal activity during homeostatic synaptic plasticity in vivo, we examined the IL-33 protein expression in hippocampal astrocytes in response to visual deprivation. Dark rearing, a form of visual deprivation that globally decreases neuronal activity in the visual cortex, is a well-established model for studying experience-dependent homeostatic synaptic plasticity (60–62). Emerging studies show that hippocampal neurons exhibit experience-induced molecular changes similar to those in visual cortical neurons (63, 64). Accordingly, compared to the normally reared (NR) mice, the dark-reared (DR) mice exhibited significantly decreased hippocampal neuronal activity as indicated by a decrease in Arc, whose gene expression is regulated by synaptic activity (*SI Appendix*, Fig. S11). Notably, compared to NR mice, the DR mice had a significantly greater percentage of IL-33-expressing astrocytes in the hippocampal CA1 region (Fig. 5 *H*–*J*). Thus, these results suggest that decreased visual sensory input leads to increased IL-33 expression in hippocampal CA1 astrocytes.

Astrocyte-Secreted IL-33 Is a Regulator of Homeostatic Synaptic Plasticity in the Hippocampal CA1 Microcircuitry. To determine if and how the astrocyte-secreted IL-33 regulates homeostatic synaptic plasticity in the hippocampal microcircuitry, we examined whether inhibiting IL-33/ST2 signaling in vivo affects the regulation of structural synapses in CA1 excitatory neurons following suppression of their neuronal activity. We suppressed the neuronal activity of hippocampal CA1 excitatory neurons by delivering and expressing NpHR in the neurons followed by light stimulation. Suppression of the neuronal activity of CA1 excitatory neurons significantly increased the number of dendritic spines (by 17%) 8 h after light stimulation (Fig. 6 *A*–*C*). Meanwhile, this increase was abolished by inhibiting IL-33/ST2 signaling upon administration of soluble ST2 (sST2), a decoy receptor of IL-33 (Fig. 6 *B* and *C*). In addition, suppressing the neuronal activity of pyramidal excitatory neurons in the hippocampal CA1 microcircuitry via the optogenetic activation of their neighboring ChR2-expressing PV interneurons significantly increased the number of dendritic spines in these pyramidal excitatory neurons (Fig. 6 *D*–*F*). Meanwhile, sST2 administration completely abolished the increase in the number of dendritic spines induced by neuronal activity change (Fig. 6 *E* and *F*).

To demonstrate that astrocyte-secreted IL-33 regulates structural synapses in the adult mouse CA1 hippocampus, we specifically knocked out IL-33 in CA1 astrocytes by delivering and expressing Cre recombinase in these astrocytes in 3-mo-old *Il33* floxed ($Il33^{fl/fl}$) mice using astrocyte-specific (gfaABC1D) promoter-driven Cre virus (Fig. 6*G*). Compared to the wild-type mice injected with Cre virus (control), the Cre-injected $Il33^{fl/fl}$ mice (i.e., IL-33 cKO) exhibited a complete loss of IL-33 protein in the GFAP-labeled CA1 astrocytes expressing Cre recombinase (Fig. 6 *H* and *I*). Importantly, these IL-33 conditional knockout mice exhibited a significant decrease (31%) in the number of VGluT1-positive PSD-95 clusters in the hippocampal CA1 stratum radiatum subregion (Fig. 6 *J* and *K*), indicating a decrease of excitatory synapses. These findings collectively suggest that astrocyte-derived IL-33 signaling is required for the formation of CA3–CA1 excitatory synapses in the hippocampal CA1 microcircuitry.

IL-33/ST2 Signaling Is Important for Memory Performance in Young Adult Mice. To determine whether the IL-33/ST2-dependent regulation of homeostatic synaptic plasticity is involved in hippocampus-associated cognitive functions, we investigated whether blockade of IL-33/ST2 signaling affects the working and contextual memory of mice by employing the Y-maze spontaneous alternation test and contextual fear conditioning test, respectively.

The Y-maze test is a measure of the spontaneous tendency of the mice to alternate their free choices to enter the two arms of the maze (65). When the arm chosen for the first entry was registered, the control C57 mice preferred the previously "unvisited" arm of the maze as the first choice and entered it more frequently (Fig. 7 *A* and *B*). In contrast, sST2-treated mice exhibited a significantly reduced preference for the unvisited arm with fewer alternations (Fig. 7 *A* and *B*). This suggests that IL-33/ST2 signaling plays a role in encoding spatial information into working memory.

In the contextual fear conditioning test, the mice were placed in a novel context and exposed to an electric foot shock (66, 67). Twenty-four hours after the foot shock, the mice were returned to the same context and tested for freezing behavior to assess the conditioning associated with the context and the foot shock. Compared to age-matched control mice (Con), sST2-treated mice exhibited 40% less freezing time 24 h after the electric foot shock (Fig. 7*C*). This suggests that blockade of IL-33/ST2 signaling impairs contextual memory formation as assessed by freezing behavior.

To confirm that sST2 administration does not affect the locomotion and/or anxiety of mice, we subjected sST2-treated mice to the open field test. There was no difference in the total distance traveled or time spent in the central and peripheral zones between the sST2-treated mice and age-matched controls (Fig. 7 *D* and *E*). Thus, the results indicate that the effect of sST2 on hippocampus-associated memory performance is independent of locomotion and anxiety. Hence, these results collectively indicate that IL-33/ST2 signaling plays an important role in learning and memory in young adult mice.

Discussion

Astrocytes plays a key role in learning and memory through the regulation of hippocampal synaptic plasticity, but the underlying molecular and cellular mechanisms remain unclear. Our study shows that IL-33 is a major astrocyte-secreted factor that regulates homeostatic synaptic plasticity in the adult mouse hippocampus and that IL-33/ST2 signaling is important for learning and memory. We found that the neuronal activity blockade-induced secretion of IL-33 is required for homeostatic synaptic plasticity in cultured hippocampal neurons. Moreover, IL-33 administration to hippocampal cultures in vitro and adult mouse hippocampus in vivo enhances hippocampal excitatory synapse formation and neurotransmission; this action is mediated through IL-33 neuronal receptor activation and PSD-95 recruitment to synapses. In addition, conditional knockout of IL-33 in hippocampal CA1 astrocytes in mice locally decreases the number of excitatory synapses, confirming the role of astrocyte-derived IL-33 in excitatory synapse formation. Furthermore, inhibiting IL-33 signaling in vivo by sST2 administration attenuates the increase of CA1 excitatory synapses induced by the optogenetic suppression of pyramidal neuronal activity and results in impaired spatial memory formation in mice.

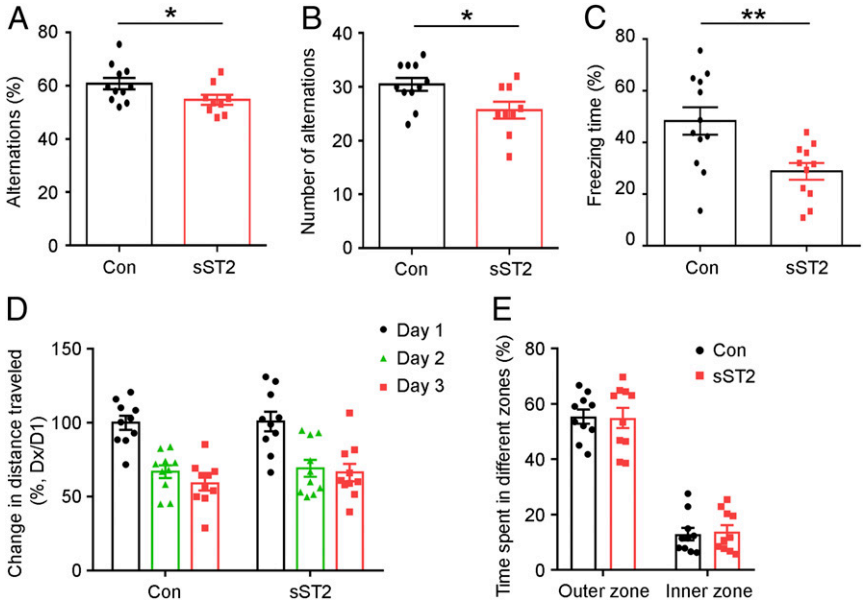

Fig. 7. IL-33/ST2 signaling is important for spatial learning and memory in young adult mice. (*A–C*) Intracerebroventricular administration of soluble ST2 (sST2) (0.26 ng/h) or human IgG Fc fragment (Con) to 3-mo-old C57 mice via miniosmotic pumps for 9 d impaired spatial learning and memory. Quantitative analysis of the percentage (*A*) and the number (*B*) of alternations in the Y-maze test (*$P < 0.05$, two-tailed unpaired *t* test; Con: $n = 11$ mice; sST2: $n = 9$ mice). (*C*) Quantitative analysis of the percentage of freezing time 1 d after electric foot shock in the contextual fear conditioning test (**$P < 0.01$, two-tailed unpaired *t* test; Con: $n = 12$ mice; sST2: $n = 11$ mice). (*D* and *E*) sST2 administration did not affect locomotor activity or anxiety-like behavior in 3-mo-old C57 mice in the open field test. (*D*) Change in distance traveled (Dx) relative to the distance traveled on the first day (D1) of training (percentage). (*E*) Time spent (percentage) in the inner zones versus outer zones in the first 5 min of open field exploration ($n = 10$ mice per group). Values are the mean ± SEM.

Hence, these findings demonstrate an important role of astrocyte-secreted IL-33 in the regulation of homeostatic synaptic plasticity in response to neuronal activity changes in the adult hippocampus.

Our study provides key insights into the molecular and cellular basis of the negative feedback mechanism involved in homeostatic synaptic plasticity. We show that inactivating hippocampal CA1 excitatory pyramidal neurons by directly suppressing their activity or activating their neighboring PV interneurons stimulates the local release of IL-33 from astrocytes, which in turn increases the synaptic excitability of these neurons. This IL-33-dependent homeostatic feedback mechanism enables CA1 pyramidal neurons to receive more inputs from CA3 presynaptic neurons, which ensures that the neural circuitry is sufficiently flexible and stable for further synaptic changes during subsequent learning experiences. Thus, our findings provide in vivo evidence showing how astrocyte-secreted factors are regulated by neuronal activity and consequently mediate the activity-dependent regulation of synaptic changes and neuronal circuit functions. As such, astrocytes have a key role in hippocampal synaptic plasticity and neural circuit adaptation.

Together with recent reports, the present study suggests that IL-33 can regulate synaptic development and functions in specific neural circuits through distinct cellular mechanisms. For example, IL-33 released from astrocytes restricts excitatory synapse formation in spinal cord development through the activation of ST2-dependent microglial synaptic pruning (29). A very recent study reports the role of neuron-derived IL-33 in enhancing excitatory synapse formation in the hippocampal dentate gyrus in adult mice through extracellular matrix clearance by microglia (68). Meanwhile, our findings reveal that IL-33 exerts a different cellular action in the hippocampal CA1 microcircuit: the activity-dependent release of IL-33 from astrocytes acts on the neuronal IL-33 receptor complex to enhance excitatory synapse formation. IL-33 exerts its synaptogenic effect by promoting the synaptic localization of PSD-95, which results in the recruitment of AMPA receptors and the subsequent strengthening of synaptic transmission (44). Therefore, in the adult hippocampus, IL-33 is likely released from distinct neural cell types in specific microcircuits—astrocytes in the CA1 hippocampal microcircuitry as reported in this study and granule neurons in the hippocampal dentate gyrus (68)—to regulate synaptic functions via the synaptic recruitment of postsynaptic scaffold proteins and through the regulation of microglial functions, respectively.

Our RNA-seq analysis shows that neuronal activity blockade increases the gene expression of several astrocyte-secreted synaptogenic factors including IL-33, Chrdl1, SPARCL1, and TNFα (*SI Appendix*, Table S1). However, the mechanisms by which astrocytes respond to changes in neuronal activity to regulate the gene expression of these synaptogenic factors remain unclear. Nonetheless, it was recently suggested that astrocytes express multiple ion channels and receptors to sense the changes in neuronal activity (18, 69); and neuronal activity changes can induce expression of astrocytic genes through mechanisms involving cAMP/PKA-dependent CREB activation (70). Interestingly, we found that the activity-dependent regulation of IL-33 is exclusively confined to the astrocytes in the hippocampal CA1 region (Fig. 1*A*). These data support that the hippocampal CA1 astrocytes may directly respond to the local synaptic activity changes and transduce the signals from synapse to nucleus for transcriptional activation. This specific regulation of IL-33 might be due to the heterogeneity of astrocytes in different hippocampal subregions, which would result in circuit- and stimulus-specific responses (19, 71). Accordingly, the processes of astrocytes in the CA1 region have more excitatory synapse contacts (18) and are more sensitive to neuronal stimulation than those in the CA3 region. A single synaptic stimulus is sufficient to activate CA1 astrocytes (72, 73), whereas a tense burst of action potentials is required to activate CA3 astrocytes (74). These distinct phenotypes and responses of CA1 astrocytes might contribute to their selective ability to increase IL-33 protein expression and secretion in response to neuronal activity blockade. Interestingly, even within the CA1 region, there are two functionally

diverse subpopulations of astrocytes distinguished by their differential expression of glutamate transporters and AMPA receptors (75). Indeed, in the present study, we only observed an increase in IL-33 protein expression in a subpopulation of CA1 astrocytes as a result of neuronal activity blockade (Figs. 1 *B* and *C* and 5 *B*–*J*). Hence, performing single-cell transcriptome profiling of hippocampal astrocytes to reveal the molecular and cellular phenotypes in hippocampal subregions might provide insights into the molecular mechanisms underlying the astrocytic control of hippocampal homeostatic synaptic plasticity. Nonetheless, the result of our IL-33 conditional knockout study confirms that IL-33 in CA1 astrocytes is important for CA3–CA1 excitatory synapse maintenance in the hippocampal circuit.

While homeostatic synaptic plasticity is important for the functional stability of neuronal circuits, neuronal activity can be chronically perturbed in many pathological conditions due to neuronal network dysregulation, which contributes to cognitive impairments in neurodegenerative diseases (76, 77). For example, patients with mild Alzheimer's disease have fewer excitatory synapses in the hippocampal CA1 region (78, 79). It has been reported that Alzheimer's disease patients also exhibited decreased IL-33 transcript levels in the brain and impaired IL-33/ST2 signaling (37, 80). While our current study shows that astrocytic IL-33 is required for maintaining hippocampal CA1 excitatory synapses and IL-33/ST2 signaling is important for hippocampal-dependent memory functions in normal adult mice, we previously reported that replenishing IL-33 in Alzheimer's disease transgenic model mice ameliorates synaptic plasticity impairment and memory dysfunctions (37). Therefore, it would be of interest to examine the roles of IL-33/ST2 signaling in cognitive dysfunctions under pathological condition.

In conclusion, our findings demonstrate that astrocyte-secreted IL-33 is important for the neuronal activity-dependent homeostatic adaptation of hippocampal CA1 synapses by modulating changes in their structure and function. Our findings not only provide valuable insights into the mechanisms underlying the astrocyte-driven neuromodulation of homeostatic synaptic plasticity but also help elucidate the dysregulated synaptic mechanisms in associated neurological diseases.

Materials and Methods

A detailed description of the applied materials and methods is given in *SI Appendix, SI Materials and Methods*.

Animals. All animal procedures were approved by the Animal Ethics Committee at The Hong Kong University of Science and Technology (HKUST) and conducted in accordance with the Guidelines of the Animal Care Facility of HKUST. See *SI Appendix, SI Materials and Methods* for details.

RNA Sequencing Analysis. We performed standard bulk RNA-seq analysis on vehicle- or TTX-treated cultured rat hippocampal cells. See *SI Appendix, SI Materials and Methods* for details.

Immunostaining and Quantitative Analysis. We used antibodies specific for IL-33, GFAP, Olig2, MAP2, PSD-95, VGluT1, GluA2, c-Fos, GFP, and EYFP as well as tdTomato and mCherry for immunostaining. See *SI Appendix, SI Materials and Methods* for details.

Electrophysiology. We performed whole-cell mEPSC recordings to examine excitatory synaptic transmission using a MultiClamp 700A amplifier (Axon Instruments). See *SI Appendix, SI Materials and Methods* for details.

Virus Injection and Optogenetic Stimulation. We injected different types of viruses into the hippocampal CA1 region in C57, PV-Cre, or *Il33*$^{fl/fl}$ mice. We analyzed synaptic changes in brain sections after virus expression with or without optogenetic manipulation. See *SI Appendix, SI Materials and Methods* for details.

Behavioral Tests. The experimenters who conducted all behavioral tests were blinded to the treatments of the tested mice. Only 3-mo-old males were used for behavioral tests. See *SI Appendix, SI Materials and Methods* for details.

Statistical Analyses. All data are expressed as the arithmetic mean ± SEM. Statistical analyses were performed using GraphPad Prism (version 8.0). The significance of differences was assessed by Student's *t* test, or one- or two-way ANOVA followed by the Tukey post hoc test as indicated. The level of significance was set at $P < 0.05$. All experiments were performed at least in triplicate unless otherwise specified.

Data Availability. All RNA-seq data discussed herein have been deposited in the NCBI Gene Expression Omnibus (GEO) database under accession no. GSE161540. In particular, the gene expression level of all proteins is provided in Dataset S1, and the gene expression level of up-regulated secreted factors is provided in Dataset S2. Other data generated from this study are included in the article and *SI Appendix*.

ACKNOWLEDGMENTS. We are grateful to Dr. Masayoshi Mishina (Ritsumeikan University), Dr. Mingjie Zhang (HKUST), and Dr. Kwok-On Lai (University of Hong Kong) for generously providing some of the expression constructs. We also thank Dr. Don Arnold (University of Southern California) and Dr. Bryan Roth (University of North Carolina at Chapel Hill) for providing expression constructs through Addgene. We thank Dr. Edward Tam, Cara Kwong, Wayne Ng, Abigail Miranda, Ka-Chun Lok, and Ryan Delos Reyes for excellent technical assistance and other members of the N.Y.I. laboratory for many helpful discussions. This study was supported in part by the Research Grants Council of Hong Kong (HKUST16124616, HKUST16149616, and HKUST16102717; Collaborative Research Fund C6027-19GF); the National Key R&D Program of China (2017YFE0190000 and 2018YFE0203600); the Area of Excellence Scheme of the University Grants Committee (AoE/M-604/16); the Theme-Based Research Scheme (T13-605/18W); the Innovation and Technology Commission (ITCPD/17-9); Guangdong Provincial Key S&T Program (2018B030336001); and the Shenzhen Knowledge Innovation Program (JCYJ20180507183642005 and JCYJ20170413173717055).

1. S. Cohen, M. E. Greenberg, Communication between the synapse and the nucleus in neuronal development, plasticity, and disease. *Annu. Rev. Cell Dev. Biol.* **24**, 183–209 (2008).
2. D. M. Bannerman *et al*., Hippocampal synaptic plasticity, spatial memory and anxiety. *Nat. Rev. Neurosci.* **15**, 181–192 (2014).
3. J. C. Magee, C. Grienberger, Synaptic plasticity forms and functions. *Annu. Rev. Neurosci.* **43**, 95–117 (2020).
4. J. Li, E. Park, L. R. Zhong, L. Chen, Homeostatic synaptic plasticity as a metaplasticity mechanism - a molecular and cellular perspective. *Curr. Opin. Neurobiol.* **54**, 44–53 (2019).
5. K. Pozo, Y. Goda, Unraveling mechanisms of homeostatic synaptic plasticity. *Neuron* **66**, 337–351 (2010).
6. G. G. Turrigiano, The self-tuning neuron: Synaptic scaling of excitatory synapses. *Cell* **135**, 422–435 (2008).
7. J. Kim, R. W. Tsien, Synapse-specific adaptations to inactivity in hippocampal circuits achieve homeostatic gain control while dampening network reverberation. *Neuron* **58**, 925–937 (2008).
8. C. M. Bird, N. Burgess, The hippocampus and memory: Insights from spatial processing. *Nat. Rev. Neurosci.* **9**, 182–194 (2008).
9. G. Neves, S. F. Cooke, T. V. Bliss, Synaptic plasticity, memory and the hippocampus: A neural network approach to causality. *Nat. Rev. Neurosci.* **9**, 65–75 (2008).
10. J. Basu, S. A. Siegelbaum, The corticohippocampal circuit, synaptic plasticity, and memory. *Cold Spring Harb. Perspect. Biol.* **7**, a021733 (2015).
11. S. Tonegawa, T. J. McHugh, The ins and outs of hippocampal circuits. *Neuron* **57**, 175–177 (2008).
12. H. K. Lee, A. Kirkwood, Mechanisms of homeostatic synaptic plasticity *in vivo*. *Front. Cell. Neurosci.* **13**, 520 (2019).
13. P. Caroni, F. Donato, D. Muller, Structural plasticity upon learning: Regulation and functions. *Nat. Rev. Neurosci.* **13**, 478–490 (2012).
14. P. Mendez, T. Stefanelli, C. E. Flores, D. Muller, C. Lüscher, Homeostatic plasticity in the Hippocampus facilitates memory extinction. *Cell Rep.* **22**, 1451–1461 (2018).
15. Y. Wu, L. Dissing-Olesen, B. A. MacVicar, B. Stevens, Microglia: Dynamic mediators of synapse development and plasticity. *Trends Immunol.* **36**, 605–613 (2015).
16. W. Croft, K. L. Dobson, T. C. Bellamy, Plasticity of neuron-glial transmission: Equipping glia for long-term integration of network activity. *Neural Plast.* **2015**, 765792 (2015).
17. N. J. Allen, D. A. Lyons, Glia as architects of central nervous system formation and function. *Science* **362**, 181–185 (2018).
18. G. Dallérac, J. Zapata, N. Rouach, Versatile control of synaptic circuits by astrocytes: Where, when and how? *Nat. Rev. Neurosci.* **19**, 729–743 (2018).
19. S. Mederos, C. González-Arias, G. Perea, Astrocyte-neuron networks: A multilane highway of signaling for homeostatic brain function. *Front. Synaptic Neurosci.* **10**, 45 (2018).
20. M. De Pittà, N. Brunel, A. Volterra, Astrocytes: Orchestrating synaptic plasticity? *Neuroscience* **323**, 43–61 (2016).
21. N. J. Allen *et al*., Astrocyte glypicans 4 and 6 promote formation of excitatory synapses via GluA1 AMPA receptors. *Nature* **486**, 410–414 (2012).

22. E. Blanco-Suarez, T. F. Liu, A. Kopelevich, N. J. Allen, Astrocyte-secreted chordin-like 1 drives synapse maturation and limits plasticity by increasing synaptic GluA2 AMPA receptors. *Neuron* **100**, 1116–1132.e13 (2018).
23. D. Stellwagen, E. C. Beattie, J. Y. Seo, R. C. Malenka, Differential regulation of AMPA receptor and GABA receptor trafficking by tumor necrosis factor-alpha. *J. Neurosci.* **25**, 3219–3228 (2005).
24. D. Stellwagen, R. C. Malenka, Synaptic scaling mediated by glial TNF-alpha. *Nature* **440**, 1054–1059 (2006).
25. K. S. Christopherson *et al*., Thrombospondins are astrocyte-secreted proteins that promote CNS synaptogenesis. *Cell* **120**, 421–433 (2005).
26. H. Pribiag, D. Stellwagen, TNF-α downregulates inhibitory neurotransmission through protein phosphatase 1-dependent trafficking of GABA(A) receptors. *J. Neurosci.* **33**, 15879–15893 (2013).
27. M. Kaneko, D. Stellwagen, R. C. Malenka, M. P. Stryker, Tumor necrosis factor-alpha mediates one component of competitive, experience-dependent plasticity in developing visual cortex. *Neuron* **58**, 673–680 (2008).
28. S. D. Greenhill, A. Ranson, K. Fox, Hebbian and homeostatic plasticity mechanisms in regular spiking and intrinsic bursting cells of cortical layer 5. *Neuron* **88**, 539–552 (2015).
29. I. D. Vainchtein *et al*., Astrocyte-derived interleukin-33 promotes microglial synapse engulfment and neural circuit development. *Science* **359**, 1269–1273 (2018).
30. T. Narahashi, J. W. Moore, W. R. Scott, Tetrodotoxin blockage of sodium conductance increase in lobster giant axons. *J. Gen. Physiol.* **47**, 965–974 (1964).
31. V. Bane, M. Lehane, M. Dikshit, A. O'Riordan, A. Furey, Tetrodotoxin: Chemistry, toxicity, source, distribution and detection. *Toxins (Basel)* **6**, 693–755 (2014).
32. J. Meinken, G. Walker, C. R. Cooper, X. J. Min, MetazSecKB: The human and animal secretome and subcellular proteome knowledgebase. *Database (Oxford)* **2015**, 2015 (2015).
33. Y. Zhang *et al*., An RNA-sequencing transcriptome and splicing database of glia, neurons, and vascular cells of the cerebral cortex. *J. Neurosci.* **34**, 11929–11947 (2014).
34. F. Y. Liew, N. I. Pitman, I. B. McInnes, Disease-associated functions of IL-33: The new kid in the IL-1 family. *Nat. Rev. Immunol.* **10**, 103–110 (2010).
35. F. Y. Liew, J. P. Girard, H. R. Turnquist, Interleukin-33 in health and disease. *Nat. Rev. Immunol.* **16**, 676–689 (2016).
36. E. Dohi *et al*., Behavioral changes in mice lacking interleukin-33. *eNeuro* **4**, ENEURO.0147-17.2017 (2017).
37. A. K. Fu *et al*., IL-33 ameliorates Alzheimer's disease-like pathology and cognitive decline. *Proc. Natl. Acad. Sci. U.S.A.* **113**, E2705–E2713 (2016).
38. Q. Sun, G. G. Turrigiano, PSD-95 and PSD-93 play critical but distinct roles in synaptic scaling up and down. *J. Neurosci.* **31**, 6800–6808 (2011).
39. R. H. Scannevin, R. L. Huganir, Postsynaptic organization and regulation of excitatory synapses. *Nat. Rev. Neurosci.* **1**, 133–141 (2000).
40. E. Kim, M. Sheng, PDZ domain proteins of synapses. *Nat. Rev. Neurosci.* **5**, 771–781 (2004).
41. M. Sheng, C. C. Hoogenraad, The postsynaptic architecture of excitatory synapses: A more quantitative view. *Annu. Rev. Biochem.* **76**, 823–847 (2007).
42. B. Z. Harris, W. A. Lim, Mechanism and role of PDZ domains in signaling complex assembly. *J. Cell Sci.* **114**, 3219–3231 (2001).
43. M. Sheng, C. Sala, PDZ domains and the organization of supramolecular complexes. *Annu. Rev. Neurosci.* **24**, 1–29 (2001).
44. M. J. Kim *et al*., Synaptic accumulation of PSD-95 and synaptic function regulated by phosphorylation of serine-295 of PSD-95. *Neuron* **56**, 488–502 (2007).
45. P. Steiner *et al*., Destabilization of the postsynaptic density by PSD-95 serine 73 phosphorylation inhibits spine growth and synaptic plasticity. *Neuron* **60**, 788–802 (2008).
46. K. Perez de Arce *et al*., Synaptic clustering of PSD-95 is regulated by c-Abl through tyrosine phosphorylation. *J. Neurosci.* **30**, 3728–3738 (2010).
47. C. D. Nelson, M. J. Kim, H. Hsin, Y. Chen, M. Sheng, Phosphorylation of threonine-19 of PSD-95 by GSK-3β is required for PSD-95 mobilization and long-term depression. *J. Neurosci.* **33**, 12122–12135 (2013).
48. Z. Qin *et al*., Adaptive optics two-photon endomicroscopy enables deep-brain imaging at synaptic resolution over large volumes. *Sci. Adv.* **6**, eabc6521 (2020).
49. G. Meng *et al*., High-throughput synapse-resolving two-photon fluorescence microendoscopy for deep-brain volumetric imaging in vivo. *eLife* **8**, e40805 (2019).
50. L. Silvestri, A. L. Allegra Mascaro, I. Costantini, L. Sacconi, F. S. Pavone, Correlative two-photon and light sheet microscopy. *Methods* **66**, 268–272 (2014).
51. R. M. Wyatt, E. Tring, J. T. Trachtenberg, Pattern and not magnitude of neural activity determines dendritic spine stability in awake mice. *Nat. Neurosci.* **15**, 949–951 (2012).
52. S. J. Barnes *et al*., Deprivation-induced homeostatic spine scaling in vivo is localized to dendritic branches that have undergone recent spine loss. *Neuron* **96**, 871–882.e875 (2017).
53. F. Zhang *et al*., Multimodal fast optical interrogation of neural circuitry. *Nature* **446**, 633–639 (2007).
54. V. Gradinaru, K. R. Thompson, K. Deisseroth, eNpHR: A Natronomonas halorhodopsin enhanced for optogenetic applications. *Brain Cell Biol.* **36**, 129–139 (2008).
55. Y. Shin Yim *et al*., Reversing behavioural abnormalities in mice exposed to maternal inflammation. *Nature* **549**, 482–487 (2017).
56. V. Gradinaru *et al*., Molecular and cellular approaches for diversifying and extending optogenetics. *Cell* **141**, 154–165 (2010).
57. T. Klausberger, P. Somogyi, Neuronal diversity and temporal dynamics: The unity of hippocampal circuit operations. *Science* **321**, 53–57 (2008).
58. B. R. Ferguson, W. J. Gao, PV interneurons: Critical regulators of E/I balance for prefrontal cortex-dependent behavior and psychiatric disorders. *Front. Neural Circuits* **12**, 37 (2018).
59. F. Zhang, L. P. Wang, E. S. Boyden, K. Deisseroth, Channelrhodopsin-2 and optical control of excitable cells. *Nat. Methods* **3**, 785–792 (2006).
60. L. Gianfranceschi *et al*., Visual cortex is rescued from the effects of dark rearing by overexpression of BDNF. *Proc. Natl. Acad. Sci. U.S.A.* **100**, 12486–12491 (2003).
61. L. A. Benevento, B. W. Bakkum, J. D. Port, R. S. Cohen, The effects of dark-rearing on the electrophysiology of the rat visual cortex. *Brain Res.* **572**, 198–207 (1992).
62. M. C. D. Bridi *et al*., Two distinct mechanisms for experience-dependent homeostasis. *Nat. Neurosci.* **21**, 843–850 (2018).
63. D. C. Haggerty, D. Ji, Activities of visual cortical and hippocampal neurons co-fluctuate in freely moving rats during spatial behavior. *eLife* **4**, e08902 (2015).
64. A. B. Saleem, E. M. Diamanti, J. Fournier, K. D. Harris, M. Carandini, Coherent encoding of subjective spatial position in visual cortex and hippocampus. *Nature* **562**, 124–127 (2018).
65. A. K. Kraeuter, P. C. Guest, Z. Sarnyai, The Y-maze for assessment of spatial working and reference memory in mice. *Methods Mol. Biol.* **1916**, 105–111 (2019).
66. J. W. Rudy, N. C. Huff, P. Matus-Amat, Understanding contextual fear conditioning: Insights from a two-process model. *Neurosci. Biobehav. Rev.* **28**, 675–685 (2004).
67. S. Maren, K. L. Phan, I. Liberzon, The contextual brain: Implications for fear conditioning, extinction and psychopathology. *Nat. Rev. Neurosci.* **14**, 417–428 (2013).
68. P. T. Nguyen *et al*., Microglial remodeling of the extracellular matrix promotes synapse plasticity. *Cell* **182**, 388–403.e15 (2020).
69. A. Araque *et al*., Gliotransmitters travel in time and space. *Neuron* **81**, 728–739 (2014).
70. P. Hasel *et al*., Neurons and neuronal activity control gene expression in astrocytes to regulate their development and metabolism. *Nat. Commun.* **8**, 15132 (2017).
71. M. Santello, N. Toni, A. Volterra, Astrocyte function from information processing to cognition and cognitive impairment. *Nat. Neurosci.* **22**, 154–166 (2019).
72. A. Panatier *et al*., Astrocytes are endogenous regulators of basal transmission at central synapses. *Cell* **146**, 785–798 (2011).
73. Y. Bernardinelli *et al*., Astrocytes display complex and localized calcium responses to single-neuron stimulation in the hippocampus. *J. Neurosci.* **31**, 8905–8919 (2011).
74. M. D. Haustein *et al*., Conditions and constraints for astrocyte calcium signaling in the hippocampal mossy fiber pathway. *Neuron* **82**, 413–429 (2014).
75. M. Zhou, H. K. Kimelberg, Freshly isolated hippocampal CA1 astrocytes comprise two populations differing in glutamate transporter and AMPA receptor expression. *J. Neurosci.* **21**, 7901–7908 (2001).
76. J. Wondolowski, D. Dickman, Emerging links between homeostatic synaptic plasticity and neurological disease. *Front. Cell. Neurosci.* **7**, 223 (2013).
77. S. Frere, I. Slutsky, Alzheimer's disease: From firing instability to homeostasis network collapse. *Neuron* **97**, 32–58 (2018).
78. B. C. Dickerson *et al*., Increased hippocampal activation in mild cognitive impairment compared to normal aging and AD. *Neurology* **65**, 404–411 (2005).
79. M. A. Yassa *et al*., High-resolution structural and functional MRI of hippocampal CA3 and dentate gyrus in patients with amnestic Mild Cognitive Impairment. *Neuroimage* **51**, 1242–1252 (2010).
80. J. Chapuis *et al*., Transcriptomic and genetic studies identify IL-33 as a candidate gene for Alzheimer's disease. *Mol. Psychiatry* **14**, 1004–1016 (2009).